Linear Elasticity of Cubic Phases in Block Copolymer Melts by Self-Consistent Field Theory

Christopher A. Tyler and David C. Morse*

Department of Chemical Engineering and Materials Science, University of Minnesota, Minneapolis, Minnesota 55455

Received September 27, 2002; Revised Manuscript Received March 13, 2003

ABSTRACT: We examine the linear elasticity of the bcc and gyroid phases of block copolymer melts with self-consistent field theory (SCFT). Linear elastic moduli for single crystals are predicted by calculating the free energies for slightly deformed crystal structures. Predicted Voight and Reuss bounds for the shear modulus of a polycrystalline material are quantitatively compared to the cubic plateau moduli found in linear viscoelastic measurements of both phases with good agreement. We also consider a model of pairwise additive interactions between "micelles" in the bcc and fcc phases and find that it predicts ratios of elastic constants consistent with those predicted by SCFT for the bcc phase, but not for the fcc phase.

1. Introduction

The viscoelastic response of microphase-separated block copolymers has been studied in some detail in the last 2 decades, including work on the classical phases of lamellae, hexagonally packed cylinders, and spheres on a bcc lattice,[1−9] the bicontinuous gyroid phase,[10−12] and the metastability of the perforated-lamellar phase.[13] It has been observed that the storage modulus G' often undergoes large changes at a phase transitions, e.g., from cylinders to gyroid or from spheres to disordered. These large changes in modulus provide an experimentally convenient way to identify the order−order (OOT) and order−disorder transitions (ODT) in an isochronal temperature ramp. The elasticity of block copolymer microstructures is also of interest as a design consideration in the development of materials, such as thermoplastic elastomers and pressure-sensitive adhesives, whose function depends on this elasticity.

Measurements of the viscoelastic response of the three-dimensionally ordered bcc and gyroid cubic phases[11,12,14,15] have shown the existence of a broad low frequency elastic plateau in the storage modulus, in a wide range of materials, which is absent from the response of the two-dimensionally periodic hexagonal phase and the one-dimensionally periodic lamellar phase. Kossuth et al. suggest that this cubic plateau modulus $G°_{\mathrm{cubic}}$ is an essentially static elastic property, whose magnitude reflects the free energy cost of deforming the unit cell of these soft three-dimensional crystals.[12] Kossuth et al. showed by dimensional analysis that an SCFT calculation for this elastic modulus in an hypothetical set of corresponding states, with equal values of the interaction parameter χN, volume fraction f, and block asymmetry α, would yield a constant value for the dimensionless modulus $G°_{\mathrm{cubic}}V/RT$, where V is the copolymer molar volume. Their experimental measurements of $G°_{\mathrm{cubic}}$ for a variety of different copolymers, which formed a rough approximation to such a set of corresponding states, showed roughly constant values of $G°_{\mathrm{cubic}}V/RT \sim 0.1-0.3$ in both the gyroid and bcc phases, over a wide range of molecular volumes. Sebastian et al.[15] find a similar range of values for $G°_{\mathrm{cubic}}V/RT$ in bcc-forming melts and concentrated solutions.

Previous theoretical efforts in calculating the elastic moduli of block copolymer melts have focused on the lamellar[16,17] and hexagonal[18,19] phases and have been limited either to the weak segregation or strong segregation limits, with the exception of the method proposed by Yeung et al., which can be applied to all phases of interest at all segregation limits. In this article, we present SCFT calculations of the elastic moduli for bcc and gyroid-forming block copolymer melts, and their dependence upon molecular parameters. We compare our predictions to experimental measurements of the elasticity of bcc and gyroid-forming block copolymer melts, including those of Kossuth et al.[12] We also examine the ability of a model in which the free energy is controlled by pairwise additive interactions between micelles to describe the predicted elasticity of bcc and fcc phases.

2. Elastic Moduli from SCFT

2.1. Elasticity of Cubic Phases. The cubic phases of interest are three-dimensionally periodic structures, with unit cells defined by Bravais lattice vectors $\mathbf{a}_\mu$, with $\mu = 1, 2, 3$. To calculate the response of such a crystal to a macroscopic deformation, we calculate the change in free energy under a finite deformation tensor $\mathbf{P}$, such that the Bravais lattice vectors undergo an affine deformation

$$\mathbf{a}_\mu \rightarrow \mathbf{P}\cdot\mathbf{a}_\mu \tag{1}$$

The variation of the total free energy of a crystal to harmonic order in the strain is

$$\delta F(\epsilon) = \frac{1}{2} V \epsilon_{ij} K_{ijkl} \epsilon_{kl} \tag{2}$$

where K_{ijkl} is the fourth-order tensor of elastic moduli,

$$\epsilon_{ij} = \frac{1}{2}(\delta P_{ij} + \delta P_{ji}) \tag{3}$$

is the linear strain tensor, $\delta \mathrm{P} \equiv \mathrm{P} - \mathrm{I}$, and the sum over repeated indices is implicit. Differentiating this free energy with respect to strain yields a corresponding linear stress−strain relationship $\sigma_{ij} = K_{ijkl}\epsilon_{kl}$. The tensor K_{ijkl} must be invariant under interchange of dummy indices i and j, of k and l, and of the pairs ij and kl, as

10.1021/ma0256946 CCC: $25.00
Published on Web 04/25/2003

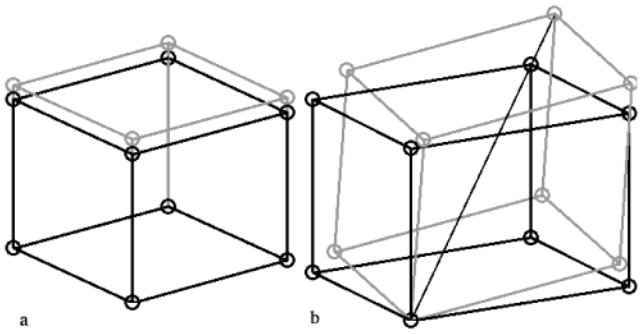

Figure 1. High-symmetry deformations of the cubic symmetry: extension along the *z*-axis (a) and a volume preserving extension along the 3-fold axis (b).

well as under all of the point group symmetries of the crystal. For a cubic crystal, K_{ijkl} contains three unique elastic moduli, K_{11}, K_{12}, and K_{44}, where $K_{11} = K_{iiii}$, $K_{12} = K_{iijj}$, $K_{44} = K_{ijij}$, with i and j being two unequal Cartesian indices.[20] The bulk modulus is $3(K_{11} + 2K_{12})$; the shear modulus, K_{44}; and the extensional modulus, K_{12}. Note that the "bulk modulus" considered here is a measure of the change in free energy caused by an isotropic change in the crystal domain spacing at constant polymer density, and not the bulk modulus of the polymer melt, which is treated as incompressible. For a completely isotropic solid, K_{ijkl} is characterized by two Lamé coefficients, λ and μ, and $K_{ijkl} = \lambda\delta_{ij}\delta_{kl} + \mu(\delta_{ik}\delta_{jl} + \delta_{il}\delta_{jk})$. A cubic crystal is isotropically elastic when $K_{11} = K_{12} + 2K_{44}$, with $K_{44} = \mu$, $K_{12} = \lambda$.

We calculate linear elastic moduli by calculating the SCFT free energies of crystals with Bravais lattices that are slightly deformed from those of the equilibrium cubic structures of interest, allowing the structures to re-equilibrate after deformation, and numerically calculating the second derivative of free energy with respect to strain. To calculate the three moduli of a cubic crystal, we must subject the crystal to three independent types of deformation. The spectral method that we use to solve the SCFT equations relies upon the use of basis functions with the space group symmetry of the phase of interest. This method requires fewer basis functions, and less computer time, to resolve structures characterized by larger symmetry groups. The bcc and gyroid structures of interest here belong to space groups $Im\bar{3}m$ (bcc) and $Ia\bar{3}$d (gyroid), respectively, both of which contain 48 symmetry operations. An arbitrary deformation of an initially cubic structure, however, produces a deformed crystal with almost no space group symmetry. To preserve the computational advantages of this method, we use three deformations that preserve as large a subgroup of the cubic space groups of the undeformed crystals as possible: (1) isotropic dilation of the cubic lattice, which preserves all 48 symmetry operations of both phases, and yields the bulk modulus, (2) extension along the [001] axis (see Figure 1a), which preserves 16 symmetry operations in either phase and yields K_{12}, and (3) a volume preserving extension along the [111] axis (see Figure 1b), which preserves 12 symmetry operations and yields K_{44}.

To determine the isotropic elastic properties of a macroscopic polycrystalline sample, one must take an appropriate average of the elements of K_{ijkl}. Rigorous bounds on the average shear modulus of a macroscopically isotropic polycrystalline sample are given by the Voight and Reuss averages, which represent averages in which crystallites with different orientations are subjected to a common strain and a common stress, respectively.[21] For a cubic crystal, the Voight and Reuss shear moduli are

$$G_V = \frac{1}{5}(K_{11} - K_{12} + 3K_{44}) \tag{4}$$

$$G_R = \frac{5K_{44}(K_{11} - K_{12})}{3(K_{11} - K_{12}) + 4K_{44}} \tag{5}$$

In what follows, experimental measurements for the plateau value $G°_{cubic}$ and the dynamic storage modulus G' in unaligned samples will be compared to these bounds.

A somewhat wider range of values for the apparent shear modulus than that between the Voight and Reuss bounds could be obtained in simple shear deformations of single crystals with arbitrary orientations. For cubic crystals with $K_{12} + 2K_{44} > K_{11}$, which is found to be the case for all of the systems studied here, the maximum possible apparent shear modulus is $G = K_{44}$, which would be measured in simple shear deformation of a crystal whose [001] and [010] axes lie parallel to the rheometer velocity and velocity gradient directions.

2.2. Self-Consistent Field Theory. Self-consistent field theory is a statistical-mechanical mean field theory for inhomogeneous systems of flexible polymers. We refer the reader to a recent review for a physically motivated derivation,[22] and here we only summarize the results. The theory characterizes a block copolymer melt in terms of a constrained partition function $q(\mathbf{r}, s)$, which is the partition function of a segment of polymer chain of length sN, where N is the overall degree of polymerization and s is an index from 0 to 1, in which the end of the chain (monomer sN) is constrained at $\mathbf{r}$. For a diblock copolymer with a volume fraction f of monomer type A, $q(\mathbf{r}, s)$ satisfies the modified diffusion equation,

$$\partial q(\mathbf{r}; s)/\partial s = \begin{cases} \frac{1}{6}Nb_A{}^2\nabla^2 q(\mathbf{r}; s) - \omega_A(\mathbf{r})q(\mathbf{r}; s); & s < f \\ \frac{1}{6}Nb_B{}^2\nabla^2 q(\mathbf{r}; s) - \omega_B(\mathbf{r})q(\mathbf{r}; s); & s > f \end{cases} \tag{6}$$

and the initial condition $q(\mathbf{r}, 0) = 1$, where b_i is the statistical segment length and $\omega_i(\mathbf{r})$ is the chemical potential field for block i. The chemical potential field follows the Flory−Huggins form

$$\omega_A(\mathbf{r}) = \chi N\phi_B(\mathbf{r}) + \xi(\mathbf{r}) \tag{7}$$

where χkT is the energetic cost of inserting a monomer of type A into pure B and ξ is a Lagrangian pressure field chosen to satisfy the constraint of constant density, $\phi_A(\mathbf{r}) + \phi_B(\mathbf{r}) = 1$. The local volume fraction of monomers of type A is

$$\phi_A(\mathbf{r}) = \frac{1}{Q}\int_0^f \mathrm{d}s\, q(\mathbf{r}, s)q^\dagger(\mathbf{r}, s) \tag{8}$$

where Q is the unconstrained partition function

$$Q = \frac{1}{V}\int_V \mathrm{d}\mathbf{r}\, q(\mathbf{r}, 1) \tag{9}$$

and where $q^\dagger(\mathbf{r}, s)$ is the constrained partition function of the other end of the chain, satisfying eq 6 with the

right-hand side multiplied by −1 and the initial condition $q^{\dagger}(\mathbf{r}, 1) = 1$. The total Helmholtz free energy of a system of n chains is

$$\frac{F}{nkT} = -\log Q + \frac{1}{V}\int d\mathbf{r}[\chi N\phi_A(\mathbf{r})\phi_B(\mathbf{r}) - \sum_{i=A,B}\omega_i(\mathbf{r})\phi_i(\mathbf{r})] \quad (10)$$

The resulting free energy per polymer F/nkT depends only on f, χN, and the ratio of statistical segment lengths $\alpha = b_A^2/b_B^2$. As discussed by Kossuth et al.,[12] differentiation of this free energy with respect to strain yields values for the reduced elastic moduli $K_{ijkl}V/RT$, where V is the polymer molar volume, that depend on the same three dimensionless parameters.

We solve the SCFT equations by the spectral method of Matsen and Schick,[23] in which one expands all spatially varying functions in basis functions $f_i(\mathbf{r})$ that are eigenvalues of the Laplacian, so that $\nabla^2 f_i(\mathbf{r}) = -E_i f_i(\mathbf{r})$, and that have the periodicity and space group symmetry of the phase of interest. This method provides an efficient description of very symmetric structures by reducing the number of basis functions required: the use of symmetric basis functions instead of plane waves (which would be required for a periodic structure with no space group symmetry) reduces the number of basis functions by a factor approximately equal to the number of symmetry operations in the space group. The computation time required by our algorithm scales approximately as the number of basis functions cubed, and so, for the bcc and gyroid phases, this reduces the required computer time by approximately 48^3, or about 10^5. We calculate the free energy of both the undeformed and deformed structures to an accuracy of 10^{-6} kT per molecule, requiring 400−600 basis functions in the undeformed state, 1000−2000 basis functions in the deformed state. This gives our calculated elastic moduli accuracy of 1−5%. The feasibility of our use of the spectral method to describe deformed crystals thus relies crucially on the use of high-symmetry deformations, and on the construction of basis functions that exploit the remaining symmetry of the deformed crystals. In Appendix A, we discuss a method used to automatically identify the space group of a deformed crystal. In Appendix B, we discuss a method to automatically construct periodic basis functions for an arbitrary space group.

3. Elasticity of bcc and Gyroid Phases

3.1. SCFT Predictions. We have calculated the elastic behavior of block copolymer melts in the bcc and gyroid phases using the procedure outlined above. In Figure 2, we plot δF, the difference in free energy between the undeformed and deformed structure, vs the scalar deformation ϵ for bcc in the [001] and [111] deformations ($f = 0.25$, $\chi N = 17.2$, $\alpha = 1$) and for gyroid in the [001] deformation ($f = 0.40$, $\chi N = 14.7$, $\alpha = 1$). For bcc, the elastic response is within 15% of linear out to 28% strain in both extension and compression for the [001] deformation, and within 30% and 50% of linear at 10% strain in compression and extension, respectively, for the [111] deformation. For gyroid, the elastic response is also within 15% of linear out to 25% and 8% strain in compression and extension, respectively. We have been unable to calculate the free energy of the gyroid structure, either in the [001] deformation in extensions greater than 8% or in the [111] deformation in extensions greater than 4% strain or compressions greater than 1%, and are investigating whether the numerical instability has a physical origin.

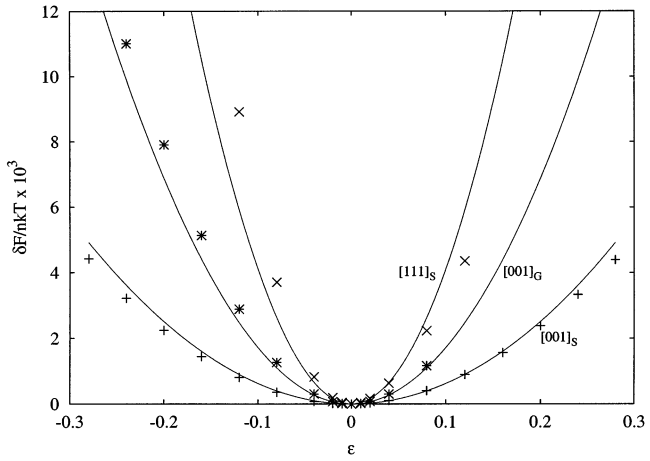

Figure 2. Change in free energy upon deformation for bcc phase under the [001] and [111] deformations and for gyroid phase under the [001] deformation.

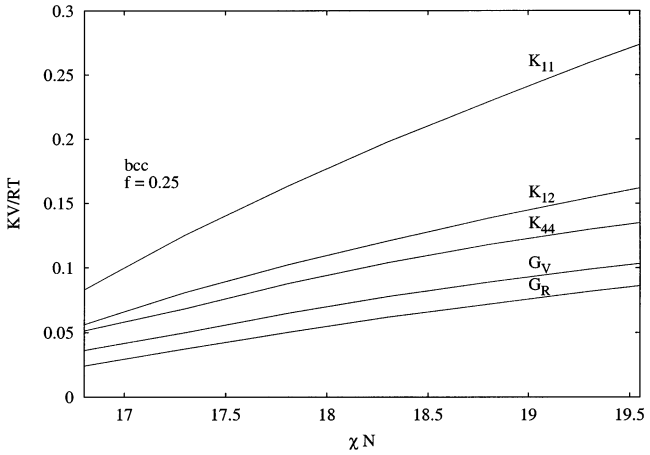

Figure 3. Elastic constants for an idealized diblock ($\alpha = 1$) as a function of χN across the phase window for the bcc phase ($f = 0.25$).

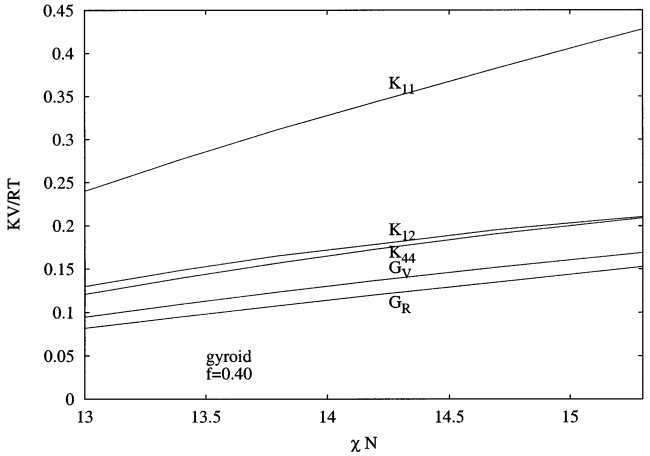

Figure 4. Elastic constants for an idealized diblock ($\alpha = 1$) as a function of χN across the phase window for the gyroid phase ($f = 0.40$).

Figures 3 and 4 show the variation of reduced elastic moduli as functions of χN for diblock copolymers with identical statistical segment lengths ($\alpha = 1$) for a bcc

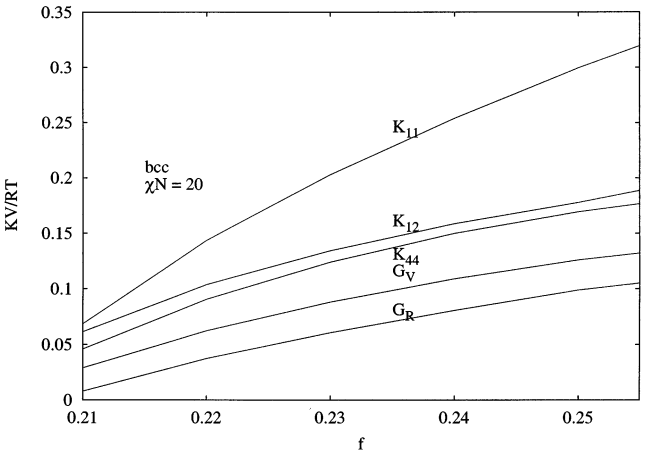

Figure 5. Elastic constants for an idealized diblock ($\alpha = 1$) as a function of f across the phase window for the bcc phase ($\chi N = 20.0$).

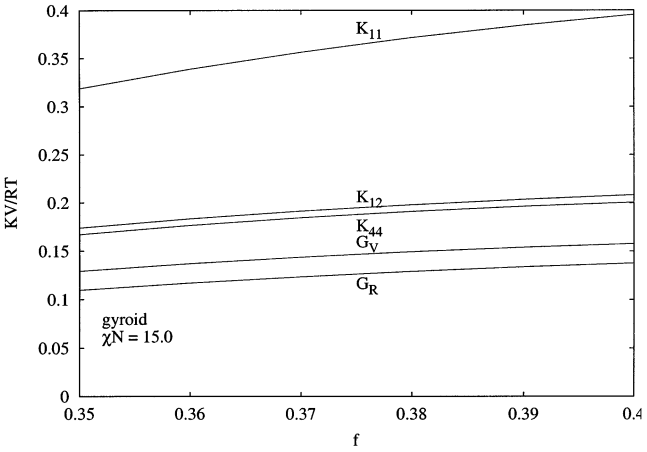

Figure 6. Elastic constants for an idealized diblock ($\alpha = 1$) as a function of f across the phase window for the gyroid phase ($\chi N = 15.0$).

phase with $f = 0.25$ and a gyroid phase with $f = 0.40$, respectively. The ranges of values shown for the parameter χN in these figures, and for f in Figures 5 and 6 correspond, in each case, to the range of values for which the phase is predicted to be thermodynamically stable. The ratios of different moduli seen here are typical of all bcc and gyroid structures considered in our calculations, with $K_{12} \approx K_{44}$ and $K_{11} \approx 2K_{44}$. The Voight and Reuss moduli vary by factors of 2−3 over the phase window for both bcc and gyroid systems.

Figures 5 and 6 show reduced moduli as functions of f for bcc and gyroid phases with $\alpha = 1$ at $\chi N = 20$ and $\chi N = 15$, respectively, calculated across the phase windows. Note that the elastic moduli vary much more strongly with f in the bcc phase, for which the Reuss modulus G_R extrapolates to zero at a point slightly beyond the order−disorder transition, than in the gyroid phase, for which we find only a 30% variation across the phase window.

Figures 7 and 8 show the variation of the elastic moduli with block asymmetry α, across the experimentally accessible range of values, for the bcc phase with $\chi N = 20$ and $f = 0.23$ and the gyroid phase with $\chi N = 15$, $f = 0.37$. There is a slight dependence on α in all of the elastic constants, accounting for a 50% variation in the elastic response.

3.2. Comparison to Experiments. The dynamic storage modulus is frequently measured as a function

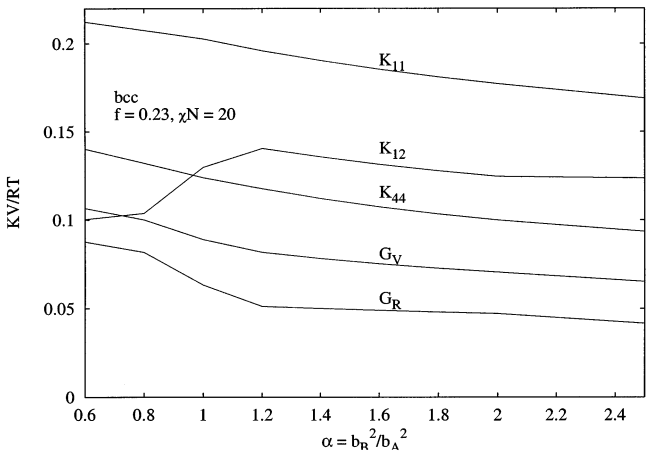

Figure 7. Elastic constants as a function of block asymmetry α for the bcc phase ($f = 0.23$, $\chi N = 20.0$).

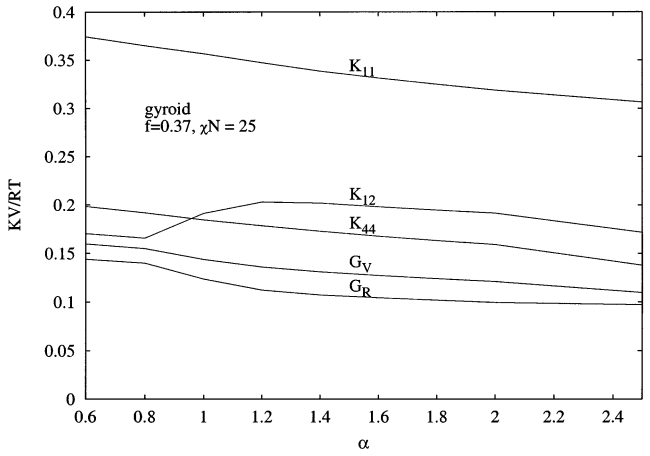

Figure 8. Elastic constants as a function of block asymmetry α for the gyroid phase ($f = 0.37$, $\chi N = 15.0$).

of temperature to determine order−disorder temperatures and/or order−order temperatures for a given copolymer. Such measurements are available for many systems exhibiting both bcc[5,10,11,24] and gyroid phases.[10,11,13,25−29] In this section, we compare our calculated elastic moduli to such temperature sweeps and to the plateau moduli published by Kossuth et al.[12] In doing so, we carry out the SCF calculations for each system using experimental values of the block asymmetry α, calculated from published values of the polymer densities and chain dimensions.[30] We have chosen a few systems for this comparison for which: (i) absolute magnitudes of $G'(T)$ at fixed frequency have been published (i.e., for which an isochronal temperature sweep has been presented in Pascal, rather than arbitrary units), (ii) for which the thermodynamic behavior has been heavily studied, so that there exist reliable values for $\chi(T)$, and (iii) for which Kossuth et al. also report a value for the plateau modulus. We assume in most cases that measurements of the dynamic storage modulus are measurements of the average properties of an isotropic sample, and compare the measurements to the Voight and Reuss moduli.

3.2.1. bcc Temperature Sweeps. For the bcc phase, we compare our calculations to the dynamic storage moduli of a PE−PEE (polyethylene-*b*-polyethylethylene) copolymer ($\alpha = 2.40$) studied by Zhao et al.,[10,11] PE−PEE−11D, with $f_{PE} = 0.25$, and a molecular weight of 55.6 kg/mol and a PEP−PEE (polyethylenepropylene-

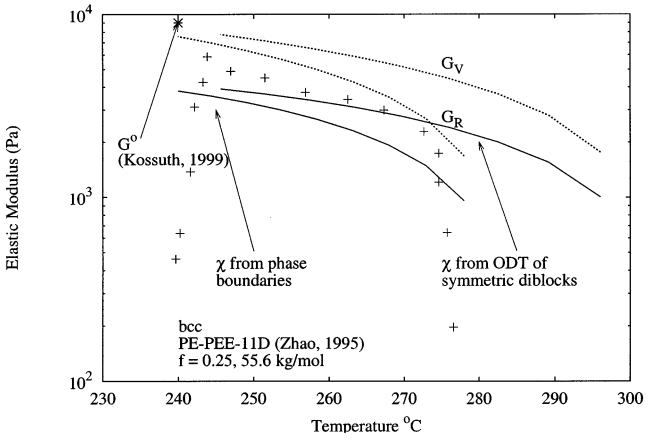

Figure 9. Comparison of the dynamic storage modulus of diblock copolymer PE−PEE−11D ($f = 0.25$, 55.6 kg/mol) upon heating at 1 °C/min, 1 rad/s, and 2−5% strain (Zhao et al. 1998), the plateau modulus $G°_{cubic}$ (Kossuth et al. 1999), and the Voight (G_V) and Reuss (G_R) moduli.

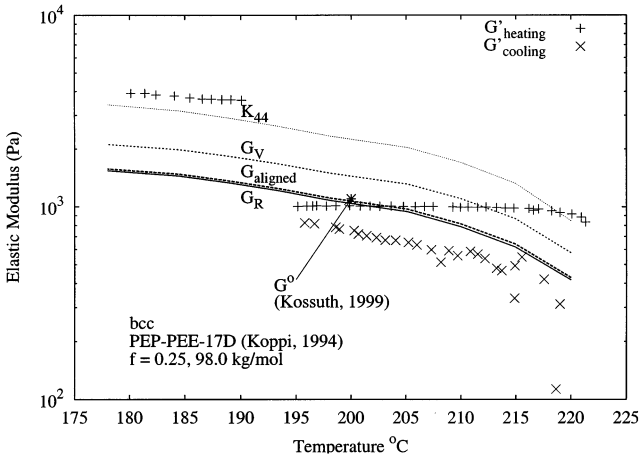

Figure 10. Comparison of the dynamic storage modulus of diblock copolymer PEP−PEE−17D ($f = 0.25$, 98.0 kg/mol) upon heating and cooling at 1 °C/min, 0.5 rad/s, and 2% strain (Koppi et al. 1994), the plateau modulus $G°_{cubic}$ (Kossuth et al. 1999), the cubic shear modulus K_{44}, the Voight (G_V) and Reuss (G_R) moduli, and $G_{aligned}$, the modulus for a single crystal with the [111] and the [110]] directions aligned with the velocity and gradient directions, respectively.

b-polyethylethylene) copolymer ($\alpha = 1.61$) studied by Koppi et al.,[5] PEP−PEE−17D, with $f_{PE} = 0.25$, and a molecular weight of 98.0 kg/mol.

We compare our predictions of the temperature-dependent elastic moduli of PE−PEE−11D to the temperature sweep published by Zhao et al.[10,11] and $G°_{cubic}$ reported by Kossuth et al.[12] in Figure 9. To predict the temperature dependence of the modulus, we have taken

$$\chi(T) = \frac{A}{T} + B$$

and chosen the constants A and B such that the experimentally observed ODT and OOT match our SCFT calculations of the phase limits for this system. This method gives $\chi(T) = 15.5/T - 0.012$ and $\chi(260\ °C) = 0.0171$, for a monomer references volume of $V_{ref} = 118$ Å^3. Cochran and Bates[31] have obtained $\chi(T) = 12.0/T - 0.0045$ and $\chi(260\ °C) = 0.0180$ for the same V_{ref} by instead measuring the ODT for $f = 0.5$ diblocks of several molecular weights and setting $\chi(T_{ODT}) = 10.5/N$. Because of the significant discrepancy in these two results for $\chi(T)$, we have compared the predictions obtained using both expressions for $\chi(T)$ in Figure 9. The temperature sweep by Zhao et al. was measured at a heating rate of 1 °C/min, at 0.5 rad/s and 2−5% strain.[10,11] Kossuth et al.'s measurement was taken at $T = 240$ °C, and is largely independent of strain amplitude and frequency. Note the factor of 2 difference between these independent measurements of G' and $G°_{cubic}$. The SCFT predictions for the Voight and Reuss moduli bracket the temperature sweep data by Zhao et al., using either expression for $\chi(T)$, but lie somewhat below the value reported by Kossuth et al. The temperature dependence predicted using the $\chi(T)$ determined by fitting to the phase boundaries is quite similiar to that seen in Zhao et al.'s data.

We compare our predictions of the temperature-dependent elastic moduli of PEP−PEE−17D to the temperature sweeps published by Koppi et al.[5] and to the value of $G°_{cubic}$ reported by Kossuth et al.[12] in Figure 10. For PEP−PEE−17D, choosing constants A and B so as to match the experimental and predicted phase boundaries yields $\chi(T) = 5.5/T - 0.0016$ and $\chi(200\ °C) = 0.010$, with $V_{ref} = 118$ Å^3. This agrees well with the expressions $\chi(T) = 4.9/T - 0.0005$ and $\chi(200\ °C) = 0.0099$ determined by Cochran and Bates[31] from measurements of the ODTs of a sequence of $f = 0.5$ diblocks, and so we show only the results obtained from our own fit to the phase boundaries in this figure. Kossuth et al.'s measurement of $G°_{cubic}$ was taken at $T = 200$ °C, and is reported to be largely independent of strain amplitude and frequency. The temperature sweep taken by Koppi et al. upon cooling (at 2 °C/min, $\omega = 0.5$ rad/s, and 2% strain, from Figure 7 of Koppi et al.) started with a disordered sample, which we would expect to produce an isotropic polycrystalline sample upon cooling below the ODT. Our predictions for the Reuss and Voight moduli are slightly above the data from this cooling sweep, with a similar temperature dependence, and bracket Kossuth et al.'s measurement.

The low temperature heating data of Koppi et al.[5] at $T < 190$ °C, which is taken from Figure 6 of Koppi et al., were measured on a sample that had been shear aligned in the cylindrical phase prior to heating into the bcc phase. This treatment was found to produce a twinned crystal with a [111] axis parallel to the flow direction and a $[1\bar{1}0]$ axis parallel to the velocity gradient direction. These data was taken after alignment by heating at 1 °C/min with an oscillatory strain at $\omega = 0.5$ rad/s and 2% strain. The higher temperature heating data, at $T > 195$ °C (taken from Figure 7 of Koppi et al., measured at 2 °C/min and identical frequency and strain rates) is also described as being data for a shear oriented sample, but gives moduli lower than those found in the lower temperature heating sweep by almost a factor of 4. We do not know the reason for this discrepancy. The predicted shear modulus for a single crystal with orientation described above is shown in the figure for comparison to this heating data, and agrees reasonably well with the higher temperature heating sweep, but is (correspondingly) significantly below that found in the low-temperature sweep.

3.2.2. Gyroid Temperature Sweeps. Our attempts to compare our predictions to experimental measurements in the gyroid phase have been complicated by the fact that the SCFT does not adequately describe the observed phase behavior of diblock copolymers near the

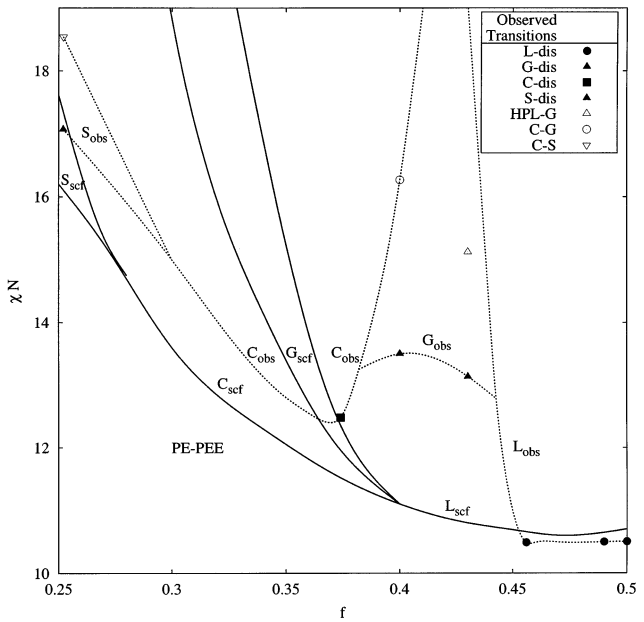

Figure 11. SCFT and experimental phase limits for PE−PEE near the gyroid phase. SCFT phase boundaries (shown in solid lines) were calculated considering the S, G, H, and L phases, but the G/H/L triple point was not rigorously identified, nor did we attempt to resolve the C/S transition for $f > 0.30$. Phase transitions upon decreasing χN, as observed by Zhao et al. (1996), are shown, with dotted lines to guide the eye.

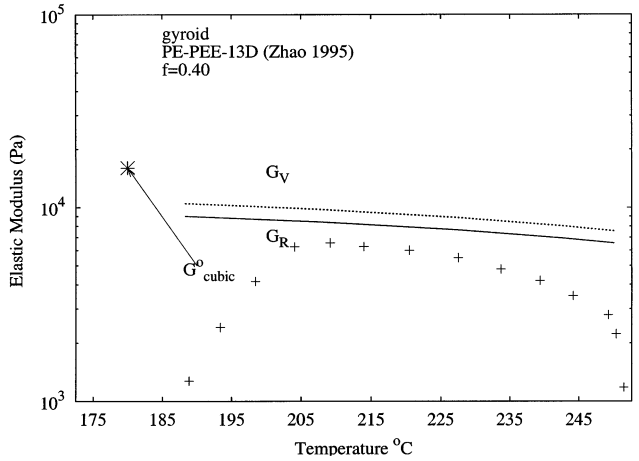

Figure 12. Comparison of the dynamic storage modulus of diblock copolymer PE−PEE−13D ($f = 0.40$, 41.5 kg/mol) upon heating at 1 °C/min, 1 rad/s, and 2−5% strain (Zhao et al. 1996), the plateau modulus $G°_{cubic}$ (Kossuth et al. 1999), and the Voight (G_V) and Reuss (G_R) moduli.

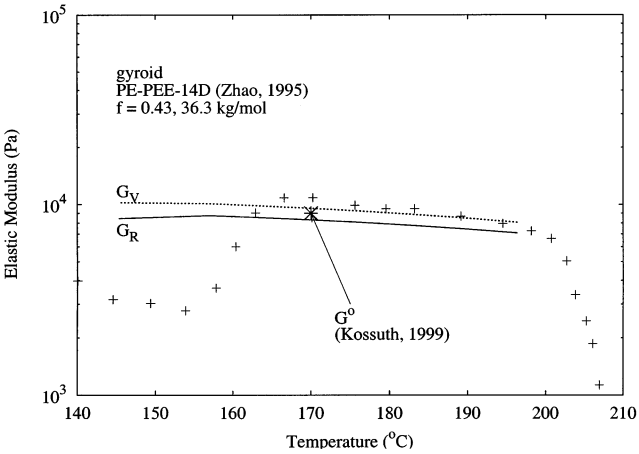

Figure 13. Comparison of the dynamic storage modulus of diblock copolymer PE−PEE−14D ($f = 0.43$, 36.3 kg/mol) upon heating and cooling at 1 °C/min, 1 rad/s, and 2−5% strain (Zhao et al. 1996), the plateau modulus $G°_{cubic}$ (Kossuth et al. 1999), and the Voight (G_V) and Reuss (G_R) moduli.

gyroid phase window. SCFT predicts that gyroid-forming copolymers will exhibit the phase sequence lamellae (L) → gyroid (G) → cylinders (C) → disorder (D) with increasing temperature or decreasing χN. It is believed that fluctuation effects, for which the SCFT does not account, become important near the ODT for nearly symmetric diblocks, stabilizing the disordered phase and suppressing the ODT.[14,32] This may explain the direct transition from gyroid to disordered phase observed in most gyroid-forming block copolymers.[5,10−13,25−27,29] In many systems, however, one also often observes a G → C transition upon *decreasing* temperature, or increasing χN.[5,12,13,23,25] This behavior is qualitatively different from that predicted by SCFT. In addition, we find for PE−PEE, as well as many of the systems studied by Kossuth et al., that the SCFT does not predict the gyroid phase to be stable in the range of copolymer compositions where it is actually observed, at any value of χN.

These discrepancies are illustrated for PE−PEE in Figure 11, in which we show the phase transitions for PE−PEE reported by Zhao et al.[10] and our SCFT predictions for the phase behavior of the same system. The SCFT predictions shown here are compared to the experiments via the relationship $\chi(T) = 12.0/T - 0.0045$ ($V_{ref} = 118$ Å) determined from the ODTs of symmetric diblocks,[31] and an asymmetry of $\alpha = 2.40$ We have calculated the SCFT phase diagram by comparing free energies of only the G, C, L, and bcc (S) phases, and have attempted to precisely locate neither the C/G/L triple point nor the C/S/L triple point (nor determine whether either exist), being more interested in the gross location and sequence of phases. We have added dotted lines to guide the eye as to the experimentally observed phases, and have included the hexagonally perforated lamellar (HPL) structure reported by Zhao et al. within the gyroid phase, to reflect the subsequent observation that the HPL phase is metastable with respect to annealing into a gyroid phase.[13] Note that SCFT predicts a gyroid phase window at significantly lower f than observed by Zhao et al., and that the *G-C* phase boundary predicted by SCFT tilts the opposite way from that inferred from experiment.

Despite the resulting ambiguities, we have compared the SCFT predictions for elastic moduli to measurements on two PE−PEE copolymers studied by Zhao et al.,[10,11] PE−PEE−13D, with $f = 0.40$ and a molecular weight of 41.5 kg/mol, and PE−PEE−14D, with $f = 0.43$ and a molecular weith of 36.3 kg/mol. As shown in Figure 11, at these volume fractions SCFT predicts the gyroid phase to be metastable, with the lamellar phase preferred. We nonetheless compare experimental results for these systems to calculations carried out for metastable gyroid phases with the measured values of f, using the same $\chi(T)$ and α as those used to calculate the SCFT phase diagram in Figure 11. Figures 12 and 13 show the measured dynamic storage modulus, the cubic plateau $G°_{cubic}$ reported by Kossuth et al.,[12] and the predicted Voight and Reuss shear moduli. The temperature sweep data for both samples, taken from Zhao et al., were measured with a 1 °C/min heating rate

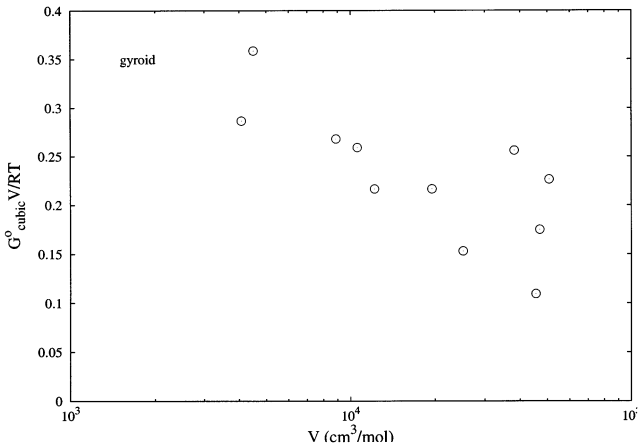

Figure 14. Dimensionless modulus $G°_{cubic}V/RT$ vs the polymer molar volume V for gyroid-forming block copolymers, adapted from Kossuth et al.[12]

at a frequency of 1 rad/s at a strain amplitude of 2−5%. The values of $G°_{cubic}$ reported by Kossuth et al. were measured at 180 and 170 °C, respectively, and are largely independent of strain amplitude and frequency. The rise and drop in $G'(T)$ correspond to the C → G OOT and the ODT. In Figure 12, the plateau modulus reported by Kossuth et al. for PE−PEE−13D is about a factor of 3 higher than the highest modulus found by Zhao et al., and the SCFT Voight and Reuss moduli lie between these values. In Figure 13, the two independent experiments agree well with each other (to within the easily identifiable experimental errors of a few tens of percent) and with our SCFT predictions.

3.2.3. Comparison to Experiments of Kossuth et al.. A broader view of elastic moduli in both the gyroid and bcc phases is provided by Kossuth et al.'s measurements of cubic plateau moduli for 17 bcc and gyroid diblock melts.[12] For the gyroid phase, their measurements yield a relatively narrow range of values for the reduced plateau modulus of $G°_{cubic}V/RT \sim 0.1-0.3$, for a set of 12 systems with molar volumes that vary over a factor of 30, as shown in Figure 14. Our SCFT predictions for the reduced Voight and Reuss bounds on the modulus of a a gyroid phase, shown in Figures 4, 6, and 8 yield a range of slightly lower values than those reported by Kossuth et al. of $GV/RT \sim 0.05-0.15$ within the range of values of χN and f for which SCFT predicts a stable gyroid phase, and over the experimentally relevant range of α. As noted above, these predictions are made at somewhat different values of f than those observed experimentally. The phase diagram shown in Figure 11 suggests that the experimental measurements may also have been taken at somewhat higher χN than the range of values shown in Figure 4, since the measurements were taken at temperatures such that $T/T_{ODT} \sim 0.90$, but the measured T_{ODT} for the gyroid phase is significantly higher than those of the neighboring lamellar and cylinder phases (for unknown reasons) and because Zhao et al. found the gyroid phase to be stable up to a temperature corresponding to $\chi N \sim 16$, somewhat above the range of values shown in Figure 4. Some of the slight difference between predicted and measured reduced moduli may thus be due to these differences in parameters.

This set of gyroid systems forms only a very rough approximation to the hypothetical set of corresponding states for which SCFT would predict a constant value of reduced modulus: the volume fraction f of the minority block range from 0.28 to 0.44; the block asymmetries α, from 0.5 to 2.4; and the ratio of T/T_{ODT}, a measure of the distance from the ODT, and hence of χN, from 0.75 to 0.98. To isolate any systematic variation of the observed reduced moduli with universal parameters, we have carried out a linear regression of $G°_{cubic}V/RT$ in terms of the variables f, α, and T/T_{ODT}; i.e., we fit the data to a model of the form $A + Bf + C\alpha + DT/T_{ODT}$. The standard deviation of $G°_{cubic}V/RT$ from this fit is 36% lower than the standard deviation from the mean value of the entire set. The remaining 64% of the scatter in $G°_{cubic}V/RT$ thus cannot possibly be accounted for by a theory that predicts a universal dependence on these parameters alone and must be due either to nonuniversalities between different chemical species, experimental error or fluctuations.

To determine the importance of fluctuations to the variations in Figure 14, we have also carried out a linear regression of $G°_{cubic}V/RT$ in terms of the fluctuation variable in Fredrickson and Helfand's fluctuation theory, $\bar{N} \propto R_o^6/V^2$, where R_o is the end to end distance of a polymer coil.[32,14] A regression of the form $G°_{cubic}V/RT = A + B/\bar{N}^m$ accounts for 43% of the variation with $m = 0.95$, suggesting that fluctuations have a significant effect upon the elastic response of the gyroid phase.

In the bcc phase, where the SCFT and observed phase behavior are more similar, our predictions for the Voight and Reuss moduli are closer to the experimental observations of the reduced moduli. Kossuth et al.[12] observed in five bcc systems with molar volumes varying by a factor of 40 that the reduced modulus ranged from $G°_{cubic}V/RT \sim 0.03-0.15$. Again, these systems also form a very rough approximation of a set of corresponding states: the minority volume fractions range from $f = 0.15$ to $f = 0.30$; the block asymmetries range from $\alpha = 0.8$ to $\alpha = 2.4$; the ratios of T/T_{ODT} range from 0.93 to 0.99. Within the range of χN and f for which SCFT predicts a stable bcc phase and over the experimentally relevant range of α, we find that the Voight and Reuss bounds yield $GV/RT \sim 0.03-0.13$.

4. Elasticity and a Pair-Potential Hypothesis

In the bcc morphology, block copolymers are gathered into micelles that have crystallized on a bcc lattice. Interactions are between the soft, corona brushes of the micelles. This physical picture suggests that the thermodynamics of the bcc (and fcc) micelle crystals might be adequately described by a model involving pairwise additive interactions between nearest neighbor micelles. This idea has been used in strong segregation to look at the phase behavior of bcc, fcc, and fluid phases of micelles.[33,34] As one test of this idea, in this section we explore the ability of a pair-potential hypothesis to explain the linear elasticity of bcc and fcc crystals.

Consider a system of micelles interacting by a pair potential $U(|\mathbf{r}|)$, where $\mathbf{r}$ is the vector connecting the centers of two neighboring micelles. The free energy of a perfect crystal of n micelles in which each micelle has z neighbors is given by $F/n = F_m + zU(R)$, where F_m is the free energy of formation of an (hypothetical) isolated micelle, which depends on f and χN, and R is the equilibrium distance between nearest neighbors. We relate the elastic modulus of such a regular lattice to the pair potential by expanding the pair potential for a single pair of neighbors with equilibrium separation $\mathbf{R}$

to second order in an arbitrary deformation $\delta\mathbf{r} = \mathbf{r} - \mathbf{R}$, as

$$U(r) = U_0 + \frac{\partial U}{\partial r_i}\delta r_i + \frac{1}{2}\frac{\partial^2 U}{\partial r_i \partial r_j}\delta r_i \delta r_j \qquad (11)$$

where i and j are Cartesian indices and summation over repeated indices is implicit. For an affine deformation $\delta r_i = \epsilon_{ij} R_j$, and for a pair potential $U(r)$ that depends only on the distance $r = |\mathbf{r}|$ between micelles, the free energy of interaction of a single pair becomes

$$U = U_0 + \frac{\partial U}{\partial r}\frac{R_i R_k}{R}\epsilon_{ik} + \left[\frac{\partial U}{\partial r}\frac{1}{R}\left(\delta_{ij} - \frac{R_i R_j}{R^2}\right)R_k R_l + \frac{\partial^2 U}{\partial r^2}\frac{1}{R^2}R_i R_j R_k R_l\right]\epsilon_{ik}\epsilon_{jl} \qquad (12)$$

It immediately follows that the elastic modulus for a periodic array of micelles with z nearest neighbors and n/V micelles per unit volume is

$$K_{ijkl} = \frac{n}{V}\sum_{\beta=1}^{z}\left[\frac{\partial U}{\partial r}\frac{1}{R}\left(\delta_{ij} - \frac{R_{\beta i}R_{\beta j}}{R^2}\right)R_{\beta k}R_{\beta l} + \frac{\partial^2 U}{\partial r^2}\frac{1}{R^2}R_{\beta i}R_{\beta j}R_{\beta k}R_{\beta l}\right] \qquad (13)$$

where β is an index for nearest neighbors. The elastic response of micelles crystallized on a lattice thus depends only on the first and second derivatives of the pair potential $U(r)$ and the number and positions of the nearest neighbors. For micelles on a bcc lattice, the three cubic elastic moduli are

$$K_{11} = \frac{1}{3}\left(\frac{\partial^2 U}{\partial r^2} + \frac{2}{R}\frac{\partial U}{\partial r}\right) \qquad (14)$$

$$K_{12} = K_{44} = \frac{1}{2}\left(\frac{\partial^2 U}{\partial r^2} - \frac{1}{R}\frac{\partial U}{\partial r}\right) \qquad (15)$$

For an fcc crystal

$$K_{11} = \frac{1}{2}\left(\frac{\partial^2 U}{\partial r^2} + \frac{1}{R}\frac{\partial U}{\partial r}\right) \qquad (16)$$

$$K_{12} = K_{44} = \frac{1}{4}\left(\frac{\partial^2 U}{\partial r^2} + \frac{1}{R}\frac{\partial U}{\partial r}\right) \qquad (17)$$

In both phases, the pair-potential model requires that $K_{12} = K_{44}$, independent of the form of the pair potential.

Figure 15 shows calculated elastic moduli as functions of χN in the bcc and fcc phases. The fcc morphology has, as expected, a higher free energy and so is metastable under these conditions. Note that while in the bcc phase $K_{12} \sim K_{44}$, this is far from true in the fcc phase. We thus find that the pair-potential model is consistent with the calculated linear elasticity of the bcc phase, but not that of the fcc phase.

5. Conclusion

We have used SCFT to calculate linear elastic moduli for the bcc and gyroid phases of diblock copolymer melts, by calculating free energies for slightly deformed crystals. The theory predicts reduced elastic moduli $K_{ijkl}V/RT$ that (as already noted by Kossuth et al.[12]) are universal functions of χN, f, and α. The reduced moduli are found to vary over factors of 2−3 with changes in χN over the stability windows in both phases. The moduli depend only weakly on f in the gyroid phase, but depend more strongly on f in the bcc phase, where the predicted shear moduli extrapolate to zero at a point slightly beyond the transition between bcc and disordered phases.

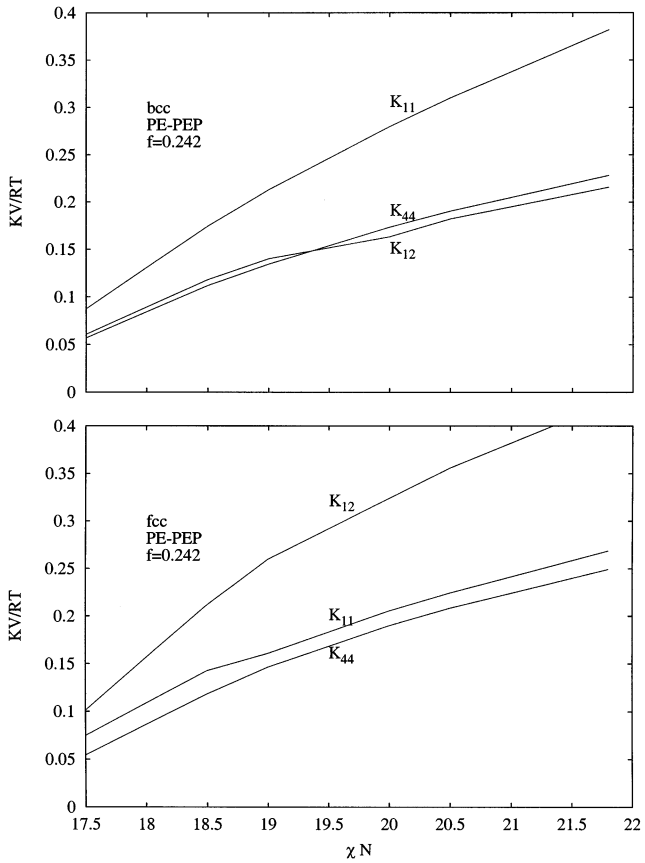

Figure 15. Calculated elastic moduli for bcc and fcc phases in a diblock with $f = 0.242$, $\alpha = 0.672$, resembling a PE−PEP diblock, calculated over the bcc phase window. While $K_{12} = K_{44}$ for the bcc phase, as predicted by a pair-potential hypothesis, $K_{12} \approx 2K_{44}$ for the fcc phase.

For comparison to experiment, we calculate Voight and Reuss bounds for the shear modulus of a polycrystalline sample. This yields a range of possible values, but we find that the width of this range is generally less than the magnitude of discrepancies between experimental measurements, as discussed below. We find reduced Voight and Reuss bounds of order $GV/RT \sim 0.1$ both for gyroid phases with $f \simeq 0.4$ and for bcc phases with $f \simeq 0.25$, which is roughly consistent with the range of values found by Kossuth et al.[12] and Sebastian et al.[15] Detailed comparisons of our predictions with linear viscoelastic measurements on a few samples show that the predictions are consistently within about a factor of 2 of experimental results for the cubic plateau modulus, with no adjustable parameters, and show a variation with temperature similar to that seen in experiment. This level of agreement is sufficient to verify that the plateau moduli seen in these experiments are essentially static moduli, resulting from deformation of the crystal unit cell, in which each chain per unit volume contributes about $0.1kT$ to the modulus, and to demonstrate that equilibrium SCFT can predict these moduli.

Our attempts to make a more precise comparison of theory and experiment have been complicated both by apparent inconsistencies in the available experimental data and by a failure of SCFT to adequately describe the phase diagram of block copolymers near the gyroid window. Regarding the experiments, we repeatedly find that independent measurement of the elastic moduli on identical samples differ by factors of 2. We do not know the reasons for these discrepancies, but we recognize that they may be due in part to different sample preparation, resulting in different crystal alignments within the sample, as well as the fact that some of these data were originally taken to identify phase boundaries, for which a very accurate measurement of the modulus is not necessary. Regarding the failures of theory, for the case of PE−PEE that we studied in detail, experiments find a transition from gyroid to cylindrical upon cooling, rather than upon heating as predicted by SCFT and find the gyroid phase to be stable in a composition range substantially different from that predicted by SCFT using the observed asymmetry α. The error in the predicted phase sequence for gyroid-forming polymers does not seem to have attracted much attention previously.

Both Kossuth et al.[12] and Sebastian et al.[15] found an empirical relationship $G°_{\mathrm{cubic}} \propto d^{-3}$ between their measured values of the modulus $G°_{\mathrm{cubic}}$ and the unit cell size d, with a constant of proportionality that Sebastian et al. note corresponds to about $18kT$ per micelle per unit volume. This relationship is inconsistent with the predictions of SCFT for a hypothetical set of corresponding states with equal values of χN, α and f. As discussed by Kossuth et al., SCFT predicts that such a set of states should yield a constant value of GV/RT, where the molar volume $V \propto N$, and the cell size $d \propto N^{1/2}$, and so it predicts $G \propto d^{-2}$, rather than $G \propto d^{-3}$, in this idealized situation. The ability of SCFT to quantitatively predict values for the modulus suggests that this empirical correlation, though it fits the available data, does not provide a useful basis for understanding the physical origin of the modulus.

We have tested the ability of a model of pairwise additive interactions between "micelles" to describe the elasticity of bcc and fcc crystals by comparing the ratios of cubic elastic constants predicted by the pair-potential model to those obtained from SCFT. We find that the bcc phase roughly obeys the relationship predicted by the pair-potential model, but that the fcc phase clearly does not. The failure to describe the elasticity of the fcc phase raises doubts in our minds about the ability of any pair-potential model to provide a sufficiently universal description of competing arrangements of micelles, including the micellar fluid state, near the order−disorder transition.

Acknowledgment. We thank David Giles and Gove N. Allen for useful discussions and the Minnesota Supercomputer Institute for providing the necessary computer time. This work was supported primarily by the MRSEC program of the National Science Foundation under Award Number DMR-9809864 and by a National Science Foundation graduate fellowship.

Appendix A. Space Group Symmetry

The symmetry of a crystal is specified by its Bravais lattice, which defines its periodicity, and by a group of discrete symmetry operations, such as reflections and finite rotations, which define its space group. Space group symmetries are operations of the form

$$\mathbf{r} \rightarrow \mathbf{R}_\beta \cdot \mathbf{r} + \mathbf{t}_\beta \tag{18}$$

where $\mathbf{R}_\beta$ is a transformation matrix representing a point group symmetry operation such as reflections through a plane or rotations about an axis, $\mathbf{t}_\beta$ is a vector displacement, which is usually a combination of low order fractions of the Bravais lattice vectors, and β is an index used to label different elements of the group. Point group operations are represented by operations with $\mathbf{t}_\beta = 0$, while operations involving glide planes and screw axes are represented using nonzero translations vectors. The bcc phase has space group $Im\bar{3}m$, which has 48 elements, all with $\mathbf{t} = 0$, while the gyroid phase has space group $Ia\bar{3}d$, which also has 48 elements characterized by the same set of rotation matrices as bcc, but which contains 24 elements that involve nonzero translations.

We wish to determine the space group of a deformed crystal produced by subjecting the Bravais lattice to an affine deformation $\mathbf{a}_\mu \rightarrow \mathbf{P}\cdot\mathbf{a}_\mu$. Consider two points $\mathbf{r}_1$ and $\mathbf{r}_2$ in the undeformed crystal that are related by a symmetry operation $\mathbf{r}_1 = \mathbf{R}\cdot\mathbf{r}_2 + \mathbf{t}$. We first affinely deform $\mathbf{r}_1$ to define a corresponding position in the deformed crystal

$$\mathbf{r}_1' = \mathbf{P}\cdot\mathbf{r}_1 = \mathbf{P}\cdot\mathbf{R}\cdot\mathbf{r}_2 + \mathbf{P}\cdot\mathbf{t} \tag{19}$$

If $\mathbf{r}_1'$ and $\mathbf{r}_2' = \mathbf{P}\cdot\mathbf{r}_2$ are still related by a symmetry operation characterized by a tensor $\mathbf{R}$, then

$$\mathbf{r}_1' = \mathbf{R}\cdot\mathbf{r}_2' + \mathbf{t}' = \mathbf{R}\cdot\mathbf{P}\cdot\mathbf{r}_2 + \mathbf{t}' \tag{20}$$

where $\mathbf{t}'$ is an affinely deformed translation vector. Equating eqs 19 and 20, we see that for the symmetry element to be preserved under the deformation $\mathbf{P}$, $\mathbf{R}$ and $\mathbf{P}$ must commute

$$\mathbf{R}\cdot\mathbf{P} = \mathbf{P}\cdot\mathbf{R} \tag{21}$$

and the translation vector must undergo an affine deformation $\mathbf{t}' = \mathbf{P}\cdot\mathbf{t}$. This criterion does not identify any symmetry imposed by $\mathbf{P}$, e.g., by compressing a tetragonal lattice into a cubic lattice, but only identifies symmetry operations of the original group that apply to the deformed structure.

We determine the symmetry of a deformed cubic unit cell by numerically checking which of the 48 symmetry operators for the bcc (or gyroid) space group commute with a given deformation, and then check that this new subset of operators is itself a group. For the isotropic dilation, the deformation matrix $\mathbf{P} = (1 + \epsilon)\mathbf{I}$, where $\mathbf{I}$ is the identity, preserves all symmetry. The change in free energy under this deformation is

$$\delta F = \frac{3}{2}(K_{11} + 2K_{12})V\epsilon^2$$

For the [001] deformation, the deformation matrix

$$\mathbf{P} = \begin{pmatrix} 1 & 0 & 0 \\ 0 & 1 & 0 \\ 0 & 0 & 1+\epsilon \end{pmatrix} \tag{22}$$

reduces the bcc symmetry to the $I4/mmm$ space group and the gyroid symmetry to the $I4_1/acd$ space group, and yields a change in free energy

$$\delta F = \frac{1}{2} K_{12} V \epsilon^2$$

For the [111] deformation, the deformation matrix

$$\mathbf{P} = \begin{pmatrix} 1 & \epsilon & \epsilon \\ \epsilon & 1 & \epsilon \\ \epsilon & \epsilon & 1 \end{pmatrix} \tag{23}$$

reduces the symmetry of the bcc phase to the $R\bar{3}m$ space group; gyroid, $R\bar{3}c$. The deformation yields a change in free energy $\delta F = 6K_{44}V\epsilon^2$

Appendix B. Symmetrized Basis Functions

We now show how to construct basis functions that are eigenfunctions of the Laplacian and that have a specified three-dimensional periodicity and space group symmetry. A function with some three-dimensional periodicity, and no other symmetry, may be expanded in plane waves characterized by wave vectors belonging to the reciprocal lattice of the crystal of interest. A symmetrized basis function f for a specified Bravais lattice and space group may be constructed as a sum of plane waves

$$f(\mathbf{r}) = \sum_{j=1}^{N} c_j e^{i\mathbf{G}_j \cdot \mathbf{r}} \tag{24}$$

where c_j is the complex coefficient of a plane wave with reciprocal lattice wavevector $\mathbf{G}_j$, and N is the number of plane waves in the sum. The set of wavevectors used to construct such a basis function, which we call a "star", are all members of the reciprocal lattice of the crystal, with the same squared magnitude $\mathbf{G}_j \cdot \mathbf{G}_j = E$, and are also all related by symmetry elements of the crystal space group, i.e., any two wavevectors $\mathbf{G}_j$ and $\mathbf{G}_k$ in the same star are related by at least one relation of the form

$$\mathbf{G}_j = \mathbf{G}_k \cdot \mathbf{R}_\beta \tag{25}$$

where $\mathbf{R}_\beta$ is the transformation matrix associated with one of the elements of the space group. Requiring that the sum in eq 24 satisfy the symmetry

$$f(\mathbf{r}) = f(\mathbf{R}_\beta \cdot \mathbf{r} + \mathbf{t}_\beta) \tag{26}$$

yields the condition

$$c_k = c_j e^{i\mathbf{G}_j \cdot \mathbf{t}_\beta} \tag{27}$$

relating the phases of any two wavevectors. If $f(\mathbf{r})$ is required to be a real function, then the coefficients associated with wavevectors $\mathbf{G}_k = -\mathbf{G}_j$ must be complex conjugates, $c_k = c_j^*$. If the crystal structure is also symmetric with respect to inversion, $\mathbf{r} \rightarrow -\mathbf{r}$, through some inversion center that we take as the origin, then the phase factors are also all required to be real numbers, $c_j = \pm A$, where A is the same for all members of the star, and $A = 1/\sqrt{N}$ for a normalized basis vector. By arbitrarily setting $c_j = 1$ for the first wavevector in a star, and identifying a transformation, denoted $\mathbf{R}_j$, which relates $\mathbf{G}_1$ to the wavevector $\mathbf{G}_j$ for all $\mathbf{G}_j$ in a star, of the form $\mathbf{G}_j = \mathbf{G}_1 \cdot \mathbf{R}_j$, we may thus construct a symmetric basis function

$$f(\mathbf{r}) = \frac{1}{\sqrt{N}} \sum_{j=1}^{N} e^{i\mathbf{G}_1 \cdot \mathbf{t}_j} e^{i\mathbf{G}_j \cdot \mathbf{r}} \tag{28}$$

The basis function $f(\mathbf{r})$ is necessarily real only for centrosymmetric space groups. For noncentrosymmetric space groups, a star can either be closed under inversion symmetry, such that $\mathbf{G}_j$ and $-\mathbf{G}_j$ are both in the star and $f(\mathbf{r}) = f(-\mathbf{r})$, or open. If a star is closed, the c_j are real. If a star is open under inversion and its associated basis function $f(\mathbf{r})$ is thus not symmetric under inversion, then we can identify a star with its associated basis function $f'(\mathbf{r})$ whose wavevectors are the inverses of the wavevectors associated with $f(\mathbf{r})$. Thus, with an appropriate choice of phase between the two basis functions, $f(-\mathbf{r}) = f'(\mathbf{r})$. We can then construct two real basis functions, analogous to sine and cosine functions, out of linear combinations of the inversion pairs, $f_1(\mathbf{r}) = [f(\mathbf{r}) + f'(\mathbf{r})]/\sqrt{2}$ and $f_2(\mathbf{r}) = i[f(\mathbf{r}) - f'(\mathbf{r})]/\sqrt{2}$, with $i = \sqrt{-1}$.

It is possible for two wavevectors $\mathbf{G}_j$ and $\mathbf{G}_k$ to be related by more than one symmetry element, so that, e.g.,

$$\mathbf{G}_k = \mathbf{G}_j \cdot \mathbf{R}_\beta = \mathbf{G}_j \cdot \mathbf{R}_\gamma \tag{29}$$

where $\mathbf{R}_\beta$ and $\mathbf{R}_\gamma$ are transformation matrices associated with two different symmetry elements. This occurs only in stars for which the number of wavevectors is less than the number of symmetry elements of the space group. When it occurs, it is possible for the phase relationships arising from two such symmetry elements to be incompatible, if

$$e^{i\mathbf{G}_j \cdot \mathbf{t}_\beta} \neq e^{i\mathbf{G}_j \cdot \mathbf{t}_\gamma} \tag{30}$$

If the phase relationships are incompatible, eq 27 can be satisfied only by taking $c_j = c_k = 0$. Because the coefficient of each wavevector in the star is related to every other by a phase relationship, the existence of contradictory phase relationships for any two wavevectors in the star is sufficient to require that $c_j = 0$ for every wavevector in the star, causing a cancellation of the entire star of wavevectors. Because the symmetry operators form a group, we can rewrite the second equality in eq 29 as $\mathbf{G}_j = \mathbf{G}_j \cdot \mathbf{R}_\delta$ by right multiplying both sides by $\mathbf{R}_\delta^{-1}$ (noting that each group member has its inverse, which is also a group member), where $\mathbf{R}_\delta = \mathbf{R}_\gamma \cdot \mathbf{R}_\beta^{-1}$. Thus, to identify canceled stars, it is sufficient to check for incompatible phase relationships between any one member of a star and itself: a star is canceled if there exists an operation that leaves any wavevector $\mathbf{G}_j$ invariant, so that $\mathbf{G}_j = \mathbf{R}_\beta \cdot \mathbf{G}_j$, but for which $e^{i\mathbf{G}_j \cdot t_\beta} \neq 1$.

A body- or face-centered crystal system can be represented either using (i) the reciprocal lattice appropriate to the primitive unit cell and a space group that does not include any purely translational symmetries or (ii) using a larger unit cell (e.g., simple cubic) and a larger space group that includes the purely translational symmetries relating equivalent lattices. For example, the bcc and gyroid phases may both be represented either using a primitive bcc unit cell and space groups of 48 operations, or by a simple cubic unit cell and space groups of 96 operations, where two sets of 48 operators are related by the pure translation $\mathbf{t} = (1/2, 1/2, 1/2)$. The above criterion for cancellations automatically identifies all cancellations required by a space group, including

the purely translational symmetries of the body- and face-centered crystals.

To automatically generate a collection of such basis functions, we (i) sort all of the reciprocal lattice vectors with magnitudes below some maximum value into sets of wavevectors with equal magnitudes, (ii) sort these sets into stars of vectors related by symmetries, and determine all of the symmetry elements relating each pair of wavevectors in a star, (iii) check each star for cancellations, (iv) apply eq 28 to the first wavevector in each remaining star to determine the phase factors for the other members of the star, and (v), for a noncentrosymmetric space group, group open stars that are related by inversion together to form real basis functions.

Like Matsen and Schick,[23] we construct and solve the SCFT equations by expanding $\omega(\mathbf{r})$, $q(\mathbf{r}, s)$, and $\phi(\mathbf{r})$ in a set of basis functions $f_i(\mathbf{r})$ of the type described above. The only properties of the basis functions required in this calculation are eigenvalues E_i of the equation $-\nabla^2 f_i(\mathbf{r}) = E_i f_i(\mathbf{r})$, which are given by the square-magnitude of the wavevectors in the corresponding star, and the elements of an overlap matrix

$$\Gamma_{ijk} = \frac{1}{V}\int \mathrm{d}\mathbf{r}\, f_i(\mathbf{r}) f_j(\mathbf{r}) f_k(\mathbf{r}) \tag{31}$$

The construction of the basis functions as sums of plane waves makes it relatively simple to automatically calculate the elements of Γ_{ijk}, by using the fact that $\int \mathrm{d}\mathbf{r}\, e^{i(\mathbf{G}_i+\mathbf{G}_j+\mathbf{G}_k)\cdot\mathbf{r}}$ vanishes except when $\mathbf{G}_i + \mathbf{G}_j + \mathbf{G}_k = 0$.

References and Notes

(1) Almdal, K.; Bates, F. S.; Mortensen, K. *J. Chem. Phys.* **1992**, *96*, 9122−9132.
(2) Bates, F. S.; Koppi, K. A.; Tirrell, M.; Almdal, K.; Mortensen, K. *Macromolecules* **1994**, *27*, 5934−5936.
(3) Chung, C. I.; Gale, J. C. *J. Polym. Sci. B* **1976**, *14*, 1149−1156.
(4) Colby, R. H. *Curr. Opin. Colloid Interface Sci.* **1996**, *1*, 454−464.
(5) Koppi, K.; Tirrell, M.; Bates, F. S.; Almdal, K.; Mortensen, K. *J. Rheol.* **1994**, *38*, 999−1027.
(6) Larson, R. G.; Winey, W. I.; Patel, S. S.; Watanabe, H.; Bruinisma, B. *Rheol. Acta* **1993**, *30*, 245−253.
(7) Ohta, T.; Enomoto, Y.; Hardin, J. L.; Doi, M. *Macromolecules* **1993**, *27*, 4923−4934.
(8) Okamoto, S.; Saijo, K.; Hashimoto, T. *Macromolecules* **1994**, *26*, 3753−3758.
(9) Rosedale, J. H.; Bates, F. S. *Macromolecules* **1990**, *23*, 2329−2338.
(10) Zhao, J. Phase behavior of diblock copolymer mixtures: binary diblock blends and diblock solutions. Thesis, University of Minnesota, 1995.
(11) Zhao, J.; Majumdar, B.; Schulz, M. F.; Bates, F. S.; Almdal, K.; Mortensen, K.; Hajduk, D. A.; Gruner, S. M. *Macromolecules* **1996**, *29*, 1204−1215.
(12) Kossuth, M.; Morse, D.; Bates, F. *J. Rheol.* **1999**, *43*, 167−196.
(13) Hajduk, D. A.; Takenouchi, H.; Hillmyer, M. A.; Bates, F. S.; Vigild, M.; Almdal, K. *Macromolecules* **1997**, *30*, 3788−3795.
(14) Bates, F. S.; Schulz, M. F.; Khandpur, A. K.; Förster, S.; Rosedale, J. H. *Faraday Discuss.* **1994**, *90*, 1−13.
(15) Sebastian, J. M.; Lai, C.; Graessley, W. W.; Register, R. A. *Macromolecules* **2002**, *35*, 2707−2713.
(16) Wang, Z. G. *J. Chem. Phys.* **1994**, *100*, 2298−2309.
(17) Yeung, C.; Shi, A. C.; Nooland, J.; Desai, R. C. *Macromol. Theory Simul.* **1996**, *5*, 291−298.
(18) Hamley, I. W. *Phys. Rev. E* **1994**, *50*, 2872−2880.
(19) Pereira, G. G. *J. Chem. Phys* **2002**, *117*, 1871−1885.
(20) Chaiken, P. M.; Lubensky, T. C. *Principles of condensed matter physics*; Cambridge University Press: New York, 1995; p 319 ff.
(21) Hashnin, Z.; Shtrikman, S. *J. Mech. Phys. Solids* **1962**, *10*, 343−352.
(22) Matsen, M. *J. Phys.-Condes. Matter* **2002**, *14*, R21−R47.
(23) Matsen, M.; Schick, M. *Phys. Rev. Lett.* **1994**, *72*, 2660−2663.
(24) Ryu, C. Y.; Lee, M. S.; Hajduk, D. A.; Lodge, T. P. *J. Polym. Sci. B* **1997**, *37*, 2811−2823.
(25) Förster, S.; Khandpur, A. K.; Zhao, J.; Bates, F. S.; Hamley, I. W.; Ryan, A. J.; Bras, W. *Macromolecules* **1994**, *27*, 6922−6935.
(26) Khandpur, A. K.; Förster, S.; Bates, F. S.; Hamley, I. W.; Ryan, A. J.; Bras, W.; Almdal, K.; Mortensen, K. *Macromolecules* **1995**, *28*, 8796−8806.
(27) Almdal, K.; Mortensen, K.; Ryan, A. J.; Bates, F. S. *Macromolecules* **1996**, *29*, 5940−5947.
(28) Hillmyer, M. A.; Bates, F. S.; Almdal, K.; Mortensen, K.; Ryan, A. J.; Fairclough, J. P. A. *Science* **1996**, *271*, 976−978.
(29) Schulz, M. F.; Khandpur, A. K.; Bates, F. S.; Almdal, K.; Mortensen, K.; Hajduk, D. A.; Gruner, S. M. *Macromolecules* **1996**, *29*, 2857−2867.
(30) Fetters, L. J.; Lohse, D. J.; Richter, D.; Witten, T. A.; Zirkel, A. *Macromolecules* **1994**, *27*, 4639−4647.
(31) Cochran, E.; Bates, F. S. *Macromolecules* **2002**, *35*, 7368−7374.
(32) Fredrickson, G. H.; Helfand, E. *J. Chem. Phys* **1987**, *87*, 697−705.
(33) Semenov, A. N. *Macromolecules* **1989**, *22*, 2849−2851.
(34) Dormidontova, E. E.; Lodge, T. P. *Macromolecules* **2001**, *34*, 9143−9155.

MA0256946